AMERICAN SOCIETY FOR MICROBIOLOGY | Applied and Environmental Microbiology®

ENVIRONMENTAL MICROBIOLOGY

Acetylenotrophic and Diazotrophic *Bradyrhizobium* sp. Strain I71 from TCE-Contaminated Soils

Denise M. Akob,[a] John M. Sutton,[b]* Timothy J. Bushman,[a,b] Shaun M. Baesman,[c] Edina Klein,[d]§ Yesha Shrestha,[a]◊ Robert Andrews,[a]∞ Janna L. Fierst,[e] Max Kolton,[f,g] Sara Gushgari-Doyle,[h] Ronald S. Oremland,[c]† John L. Freeman[i]

[a]U.S. Geological Survey, Geology, Energy & Minerals Science Center, Reston, Virginia, USA
[b]Department of Biological Sciences, The University of Alabama, Tuscaloosa, Alabama, USA
[c]U.S. Geological Survey, Menlo Park, California, USA
[d]Institute for Applied Biology, Department of Applied Biology, Karlsruhe Institute of Technology, Karlsruhe, Germany
[e]Biomolecular Sciences Institute, Department of Biological Sciences, Florida International University, Miami, Florida, USA
[f]French Associates Institute for Agriculture and Biotechnology of Drylands, Ben-Gurion University of the Negev, Beer Sheva, Israel
[g]School of Biological Sciences, Georgia Institute of Technology, Atlanta, Georgia, USA
[h]Department of Civil and Environmental Engineering, University of California, Berkeley, California, USA
[i]Intrinsyx Environmental, Valley Research Park, Mountain View, California, USA

ABSTRACT Acetylene (C_2H_2) is a molecule rarely found in nature, with very few known natural sources, but acetylenotrophic microorganisms can use acetylene as their primary carbon and energy source. As of 2018 there were 15 known strains of aerobic and anaerobic acetylenotrophs; however, we hypothesize there may yet be unrecognized diversity of acetylenotrophs in nature. This study expands the known diversity of acetylenotrophs by isolating the aerobic acetylenotroph, *Bradyrhizobium* sp. strain I71, from trichloroethylene (TCE)-contaminated soils. Strain I71 is a member of the class *Alphaproteobacteria* and exhibits acetylenotrophic and diazotrophic activities, the only two enzymatic reactions known to transform acetylene. This unique capability in the isolated strain may increase the genus' economic impact beyond agriculture as acetylenotrophy is closely linked to bioremediation of chlorinated contaminants. Computational analyses indicate that the *Bradyrhizobium* sp. strain I71 genome contains 522 unique genes compared to close relatives. Moreover, applying a novel hidden Markov model of known acetylene hydratase (AH) enzymes identified a putative AH enzyme. Protein annotation with I-TASSER software predicted the AH from the microbe *Syntrophotalea acetylenica* as the closest structural and functional analog. Furthermore, the putative AH was flanked by horizontal gene transfer (HGT) elements, like that of AH in anaerobic acetylenotrophs, suggesting an unknown source of acetylene or acetylenic substrate in the environment that is selecting for the presence of AH.

IMPORTANCE The isolation of *Bradyrhizobium* strain I71 expands the distribution of acetylene-consuming microbes to include a group of economically important microorganisms. Members of *Bradyrhizobium* are well studied for their abilities to improve plant health and increase crop yields by providing bioavailable nitrogen. Additionally, acetylene-consuming microbes have been shown to work in tandem with other microbes to degrade soil contaminants. Based on genome, cultivation, and protein prediction analysis, the ability to consume acetylene is likely not widespread within the genus *Bradyrhizobium*. These findings suggest that the suite of phenotypic capabilities of strain I71 may be unique and make it a good candidate for further study in several research avenues.

KEYWORDS *Bradyrhizobium*, acetylene, acetylenotrophy, microbial ecology, nitrogen fixation, soil microbiology

Editor Jeremy D. Semrau, University of Michigan-Ann Arbor

Address correspondence to Denise M. Akob, dakob@usgs.gov.

*Present address: John M. Sutton, Absci, Vancouver, Washington, USA.

§Present address: Edina Klein, Hamburg University of Technology, Institute of Technical Microbiology, Hamburg, Germany.

◊Present address: Yesha Shrestha, U.S. Food and Drug Administration, Center for Veterinary Medicine, Laurel, Maryland, USA.

∞Present address: Robert Andrews, MRIGlobal Capital Region, Gaithersburg, Maryland, USA.

The authors declare no conflict of interest.

†Deceased.

Received 19 July 2022
Accepted 12 September 2022
Published 26 October 2022

Acetylene (C_2H_2) is a trace constituent (~20 to 40 parts per trillion [ppt]) of the Earth's present atmosphere (1–3), reflecting a mix of terrestrial and marine emissions from anthropogenic, biomass burning, and unidentified biogenic sources (4–7). Acetylene is a well-known inhibitor of a variety of microbial processes, including nitrogen-fixation (8), nitrification (9, 10), methanogenesis (11), methanotrophy (12–14), and reductive dechlorination (15). Nevertheless, despite its adverse effects, some microorganisms can utilize acetylene as their primary carbon and energy source in a process called acetylenotrophy (16). To date, acetylenotrophy has only been demonstrated in 15 aerobic and anaerobic isolates; however, environmental surveys suggest an unknown larger diversity of acetylenotrophs exists (16). As acetylenotrophy could potentially influence a wide range of microbial processes, it is important to better understand acetylenotrophs' ecophysiology and impact on the microbial world.

Acetylene can be transformed by two biochemical pathways that are catalyzed by nitrogenase (N_2ase) and acetylene hydratase (AH) enzymes. These oxygen-sensitive enzymes are structurally unrelated but have low-electrochemical potential. N_2ase is found in diazotrophic (nitrogen-fixing) microbes and catalyzes the reduction of dinitrogen to ammonia. N_2ase is known to be promiscuous, as it will also reduce other triple-bonded molecules like cyanide and acetylene. The first well-characterized acetylenotroph was the anaerobe *Syntrophotalea acetylenica* DSM 3246^T (formerly *Pelobacter acetylenicus* DSM 3246^T [17]), which uses acetylene hydratase (AH; EC 4.2.1.112) to hydrate acetylene to acetaldehyde (18). The AH of *S. acetylenica*, a nonredox active enzyme, is a unique member of the dimethyl sulfoxide reductase protein family and has been extensively studied (19, 20). The *S. acetylenica* AH contains a tungsten pyranopterin cofactor (20, 21) and its catalytic activity is dependent on the presence of a strong reducing agent (e.g., titanium [III] citrate or dithionite [19, 22]). AH is encoded by the *ahy* gene and is a monomer of 730 amino acids with four domains: domain I contains a 4Fe-4S cluster coordinated by four cysteine residues; domains I, II, and IV coordinate the bis-molybdopterin guanine dinucleotide cofactors that coordinate a tungsten ion (20). AH is highly specific for acetylene and does not react with other triple-bonded molecular analogs; for a detailed description of the AH enzyme from *S. acetylenica*, see the review by ten Brink (2014) (19). Another anaerobic member of the *Syntrophotalea* genus, *Syntrophotalea acetylenivorans* SFB93^T, simultaneously expresses both AH and N_2ase and couples growth to acetylenotrophic fermentation with diazotrophy in the absence of readily bioavailable N-sources (23).

Aerobic acetylenotrophic bacterial strains were isolated and characterized from soils and sediments. These isolates can use acetylene either as the sole carbon and energy source or consume it in conjunction with low concentrations of supplemental yeast extract (24–28). The best characterized aerobic acetylenotrophs are the isolates obtained by Rosner et al. (28): *Rhodococcus opacus* strains MoAcy1 and TueAcy1, *Rhodococcus zopfii* strain TueAcy3, and *Gordonia alkanivorans* strain MoAcy2, which are all members of the phylum *Actinobacteria*. Isolate characterization indicated that aerobic acetylenotrophic activity depends on molybdenum, unlike anaerobic *Syntrophotalea* strains with a tungsten-dependent AH. Further, Rosner et al. (28) showed that the AH of these aerobic strains did not cross-react with antibodies raised for the AH of *S. acetylenica*. The lack of cross-reactivity and requirement for an alternative cofactor indicates structural heterogeneity in the enzyme and the potential for aerobic acetylenotrophs to employ an alternative mechanism for acetylene hydration.

Most environmental acetylene is anthropogenic in origin, resulting from the abiotic interaction of naturally occurring minerals (e.g., green rusts) with halogenated, unsaturated hydrocarbon contaminants like trichloroethylene (TCE) (29–32). Presumably, long-duration flow of TCE in contaminated aquifers results in the accumulation of acetylene in the subsurface, allowing for the growth of acetylenotrophic bacteria. It also explains the ease with which incubated groundwater samples taken from the TCE-polluted Naval Air Warfare Center (NAWC) study site readily metabolized acetylene in comparison with other assayed, more pristine locations (33). Indeed, a syntrophic association could be artificially established between an acetylenotroph (*S. acetylenivorans* strain SFB93^T) and

dehalogenating anaerobes like *Dehalococcoides mccartyi* (34). In this association, SFB93^T acetylenotrophic activity sustains *D. mccartyi* growth by generating metabolic products (H_2 and acetate) and by eliminating the inhibitory effect of acetylene on TCE dehalogenation (34). This work was recently followed upon using naturally occurring populations recovered from a contaminated well (36BR-A) at the NAWC site that were initially enriched for acetylenotrophs, followed by TCE addition (35). This study observed successful dehalogenation by the resident population of dehalococci, suggesting an *in situ* TCE-bioremediation strategy focused around exploiting acetylene-metabolism as an alternative to current efforts using nonspecific electron donors like molasses. In addition, 16S rRNA gene sequence-based population assessments suggested that members of the phylum *Actinobacteria* rather than *Syntrophotalea* were the acetylenotrophs in this system, which agreed with earlier attempts to isolate acetylene fermenters from freshwater Searsville Lake (33).

In this study, we evaluated the presence of acetylenotrophs in TCE-contaminated soils under a stand of poplar trees treated for TCE-phytoremediation amended with an endophytic bacterium at the National Aeronautics and Space Administration (NASA) Ames Research Center (36, 37). We isolated an aerobic acetylenotroph from the genus *Bradyrhizobium*, isolate I71, expanding the known distribution of acetylenotrophs to the class *Alphaproteobacteria*. Prior to this study, no aerobic acetylenotrophs were known to be affiliated with the *Proteobacteria* phylum. *Bradyrhizobium* sp. strain I71 was shown to couple growth to acetylene consumption and diazotrophy. Genome sequencing and analysis identified a putative AH in strain I71. Assays with other *Bradyrhizobium* isolates did not show that acetylenotrophy is ubiquitous in this genus. Expanding the known phylogenetic diversity of acetylenotrophs and identifying their AH genes may allow a better estimation of the environmental importance of these organisms.

RESULTS AND DISCUSSION

Characterization of acetylenotrophic isolate I71 from TCE-contaminated soils. Soils from a TCE-contaminated site at the NASA Ames Research Center undergoing phytoremediation were used for selective enrichment of aerobic acetylenotrophs. Acetylene was rapidly consumed in soil enrichments and activity could be sustained with repeated additions of acetylene (see Fig. S1 in the supplemental material) (38). These enrichment cultures were then used for isolation using a multipronged approach combining agar shakes, serial dilutions, and plate bottle methods. This isolation approach was necessary to ensure that selective conditions were maintained for an organism which could use acetylene (a gaseous substrate) as its primary carbon substrate. The development of the plate bottle approach (Fig. S2) allowed us to obtain an isolate via streak-plating while measuring acetylene consumption by sampling the headspace gas. The resulting acetylenotrophic isolate, strain I71, was maintained in the United States Geological Survey (USGS) Reston Microbiology Lab (RML) over several transfers in WBMMpAc liquid media and via repeated additions of acetylene (Fig. S2). WBMMpAc liquid medium is a 3-morpholinopropane-1-sulfonic acid (MOPS)-buffered mineral salts media that contains acetylene as the sole carbon substrate. Although MOPS is an organic compound, strain I71 required the presence of acetylene for growth (Fig. 1, discussed below). Isolate I71 was also capable of heterotrophic growth in modified arabinose gluconate (MAG) and yeast mannitol (YM; DSMZ medium 1070) medium. Furthermore, the ability of isolate I71 to grow acetylenotrophically was sustained between transfers from heterotrophic media to WBMMpAc with acetylene as the sole carbon substrate. Analysis of the 16S rRNA gene revealed that strain I71 is a member of the genus *Bradyrhizobium* within the class *Alphaproteobacteria*.

Acetylenotrophic growth of isolate I71 was demonstrated by an increase in optical density (OD_{600}) and cell numbers linked to consumption of acetylene in WBMMpAc liquid medium (Fig. 1). Isolate I71 consumed 22.4 $\pm$ 0.68 μmoles per bottle of acetylene in 91 h (cultures were grown in 50 mL liquid WBMMpAc medium in 100-mL serum bottles). These consumption rates corresponded to an increase in OD_{600} of 0.045 $\pm$ 0.001

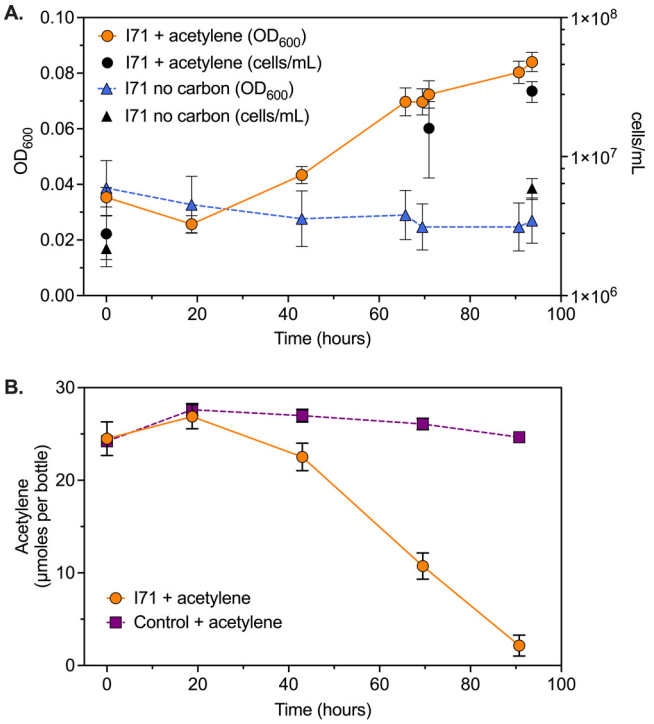

FIG 1 Growth (A) and acetylene consumption (B) in *Bradyrhizobium* strain I71 cultures. Panel A shows growth measured via optical density (OD_{600}) and cell counts (cells/mL) in cultures with acetylene (circles) or with no added carbon substrate (triangles). Panel B shows acetylene concentrations over time in the I71 culture (circle) and uninoculated controls (square) amended with acetylene. Data are averages ± standard deviation of triplicate cultures. All experiments were performed in 100-mL serum bottles containing 50 mL liquid WBMMpAc medium.

and an order of magnitude increase in cell counts. Starting cell numbers averaged $2.78\times 10^6 \pm 9.96\times 10^5$ cells/mL and increased to $2.96\times 10^7 \pm 5.08\times 10^6$ cells/mL after 94 h in cultures with acetylene (Fig. 1A). In cultures with no carbon added, average OD_{600} decreased over time while a marginal increase in cell numbers was observed ($2.08\times 10^6 \pm 5.65\times 10^5$ cells/mL at 0 h and $5.93\times 10^6 \pm 1.01\times 10^6$ cells/mL at 94 h). No acetylene loss or change in OD_{600} was observed for uninoculated medium controls (Fig. 1B and Fig. S3; [38]). Similar results were obtained when starting experiments with different starting I71 cultures (e.g., different cell lines as described in the methods) or when acetylenotrophic medium was inoculated with a culture of I71 previously grown on heterotrophic media (Fig. S4 and S5).

The maximum OD_{600} achieved by strain I71 during acetylenotrophic growth was 0.084 ± 0.003. Despite a low culture gain in density compared to many bacterial cultures, this turbidity shift was associated with nearly a 10-fold increase in bacterial cell counts. The low OD gain obtained by strain I71 is in line with the maximum OD achieved by the anaerobic acetylenotrophs, e.g., *Syntrophotalea acetylenivorans* SFB93^T and *S. acetylenica* but much lower than the OD obtained by the aerobic acetylenotroph *Rhodococcus opacus* strain TueAcy1. When grown with acetylene as the sole carbon and energy source, *S. acetylenivorans*, *S. acetylenica*, and *R. opacus* strain TueAcy1 reached maximum OD of 0.20 (23), ~0.09 (18), and ~1.0 (28), respectively. While these measurements were made at slightly different wavelengths (OD_{680} for *S. acetylenivorans*, OD_{650} for *S. acetylenica*, and OD_{578} for *R. opacus*), it is valuable to note that growth by I71 was in a similar range to the anaerobic strains. Therefore, we hypothesize that the production of acetylenotrophy byproducts, e.g., acetaldehyde (18, 39), could be inhibitory to strain I71, as was observed for *S. acetylenica* DSM 3246^T (18). Alternatively, acetylene is an inefficient substrate for growth by strain I71, or the medium may be missing essential components.

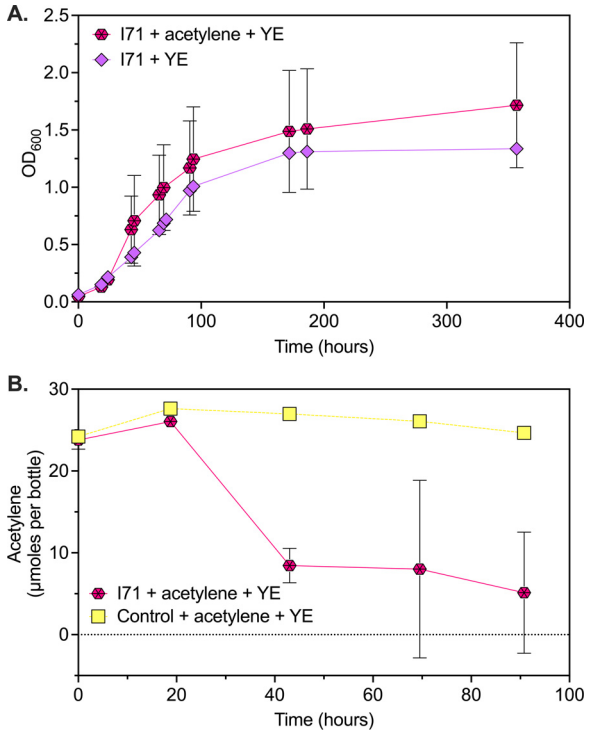

FIG 2 Heterotrophic and acetylenotrophic growth in *Bradyrhizobium* strain I71 cultures. Panel A shows growth measured via OD_{600} in cultures with acetylene and yeast extract (hexagons) or with yeast extract as the sole carbon substrate (diamonds). Panel B shows acetylene concentrations over time in the I71 culture (hexagon) and uninoculated controls (square) amended with acetylene and yeast extract. Data are averages ± standard deviation of triplicate cultures. Experiments were performed in 100-mL serum bottles containing 40 mL liquid WBMMpAc medium.

To test the latter hypotheses, strain I71 was grown in the presence of complex carbon with and without acetylene, and we compared our media composition to that used to cultivate aerobic acetylenotrophs. Isolate I71 reached similar cell densities when grown on acetylene and yeast extract compared to yeast extract alone, with cultures reaching a maximum OD_{600} of 1.72 ± 0.55 and 1.34 ± 0.003, respectively (Fig. 2A). Significantly higher culture density was achieved when I71 was grown on acetylene and yeast compared to acetylene alone ($P < 0.0001$, two-tailed *t* test). The increased culture density was linked to the consumption of acetylene, with ~15 μmoles per bottle of acetylene consumed within the first 43 h of growth (Fig. 2B). Growth with acetylene and yeast extract yielded higher cell densities compared to yeast extract alone and corresponded to an increase in OD_{600} of 0.40, indicating that growth was more favorable in the presence of a complex carbon substrate or a trace nutrient or metal in the yeast extract. No acetylene loss or change in OD_{600} was observed for uninoculated medium controls (Fig. 2 and Fig. S4; [38]). The higher cell densities achieved are more like strains in the genus *Bradyrhizobium* which reach a maximum OD_{660} of 1 when grown in a medium supplemented with yeast extract and arabinose (40) and *R. opacus* strain TueAcy1, which reaches an OD_{578} of 1 when growing acetylenotrophically (28). *R. opacus* strain TueAcy1 reached an OD_{578} of 1 when grown in the presence of 150 nM molybdate and 12 nM tungstate (28). These molybdate and tungstate concentrations were similar to those used in experiments with strain I71 (see supplemental material for detailed media recipes). Therefore, we do not believe that cofactor limitation was responsible for the low cell densities. Two additional aerobic acetylenotrophic strains were isolated in parallel with *R. opacus* strain TueAcy1: *G. alkanivorans* strain MoAcy2 and *R. zopfii* strain TueAcy3; these isolates could only grow with acetylene in the presence of 0.1% yeast extract (28). The observations suggest that although strain I71 is an acetylenotroph the strain grows

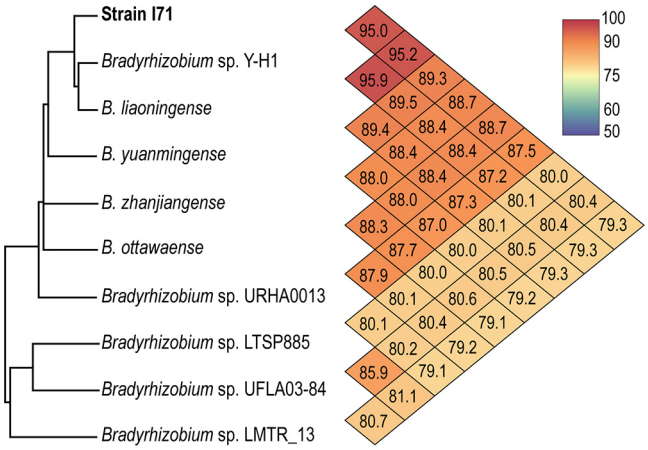

FIG 3 Heatmap and dendrogram of the average nucleotide identity over orthologous regions (OrthoANI) for genomes of *Bradyrhizobium* isolate I71 and related organisms.

best as a heterotroph and that acetylene is not an optimal sole carbon source for achieving high cell densities.

Phylogeny of *Bradyrhizobium* strain I71. Phylogenetic analysis revealed that strain I71 is a member of the genus *Bradyrhizobium* within the class *Alphaproteobacteria*. The 16S rRNA gene sequence of strain I71 was compared to the GenBank database via a BLAST search. The top 10 hits were all members of the genus *Bradyrhizobium* sharing 99.91% sequence similarity (Table S1). Strains of *Bradyrhizobium liaoningense* and *Bradyrhizobium japonicum* were among the top hits indicating that strain I71 could be affiliated with either of these species. As the phylogeny of members of the *Bradyrhizobium* is poorly resolved using 16S rRNA genes (41, 42), we confirmed strain I71's placement using genome-inferred phylogenetics. Phylogenetic inference based on 92 bacterial core genes showed that the closest relatives of I71 were *Bradyrhizobium* sp. Y-H1 and *B. liaoningense* (Fig. S6). OrthoANI values comparing I71 to other strains of *Bradyrhizobium* indicated that our isolate is unique from other sequenced isolates in the genus (Fig. 3). Strain I71 is most closely related to *B. liaoningense* CCNWSX0360 (95.2% identical via OrthoANI; Fig. 3); this value sits right on the 95 to 96% cutoff accepted to delineate species (43).

The diverse, soil-dwelling genus *Bradyrhizobium* is well known for its ability to nodulate with legumes (44) and fix nitrogen (45). This symbiotic relationship with legumes is of significant agricultural importance and has resulted in multiple well-characterized members of the genus (44), including strains of *B. liaoningense* and *B. japonicum* (Table S1). However, the lifestyles of this genus are varied; while the strains mentioned above live symbiotically with legumes, other strains are free-living in soil and may lack nitrogen-fixation and nodulation genes (46), and some members even have photosynthetic capabilities (47).

The phylogenetic placement of strain I71 within the class *Alphaproteobacteria* makes it the first observation of an acetylenotroph from within this class and further, the first known acetylenotroph in the phylum *Proteobacteria*. The most closely related acetylenotrophs are anaerobes from the *Desulfobacterota* phylum (*S. acetylenica* DSM 3246^T [18] and *S. acetylenivorans* SFB93^T [48]), which were initially members of the class *Deltaproteobacteria*, but recently reclassified into the phylum *Desulfobacterota* (17). These anaerobic acetylenotrophs use a tungsten-dependent acetylene hydratase (AH) to catalyze the first step in acetylenotrophy, hydration of acetylene (18, 23). Prior to the isolation of *Bradyrhizobium* sp. strain I71, aerobic acetylenotrophic isolates were only identified from the phyla *Actinobacteria* and *Firmicutes* (16) but little characterization of their acetylenotrophic activity was documented. Four of the aerobic acetylenotrophs from the *Actinobacteria* phylum were shown to have an AH that preferred a molybdenum cofactor over tungsten and structurally differed from the AH of *S. acetylenica* DSM 3246^T (28). Strain I71 was isolated and routinely grown only in

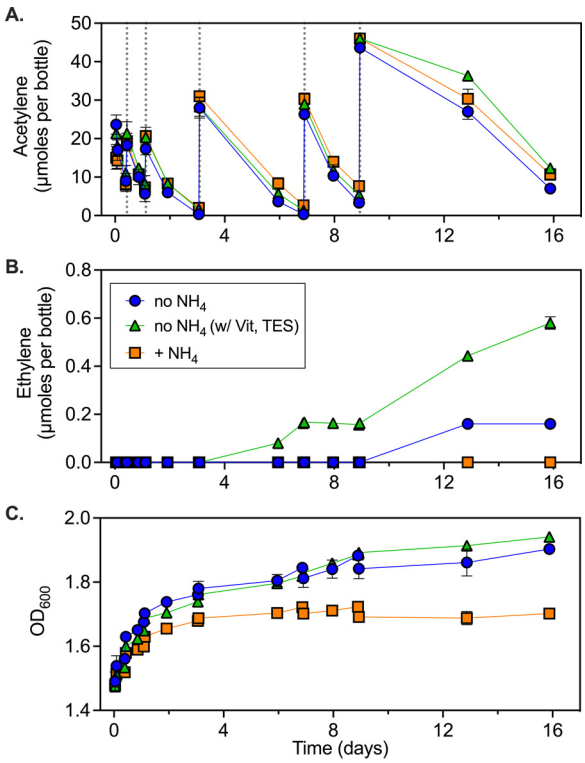

FIG 4 Acetylenotrophic and diazotrophic activity in washed and concentrated cells of *Bradyrhizobium* strain I71. (A) Consumption of acetylene, which after depletion was readded to the gas phase at intervals indicated by dashed lines. (B) Ethylene accumulation indicating nitrogenase activity. (C) Cell density as measured by OD_{600}. Symbols represent the mean of triplicate cultures and bars indicate ± 1 standard deviation. All experiments were performed in 5 mL of liquid WBMMpAc medium in 30-mL Balch tubes.

the presence of molybdenum. Therefore, we infer that the enzyme is more similar to the AH of the *Actinobacteria* isolates than that of *Syntrophotalea*.

Nitrogen fixation by *Bradyrhizobium* sp. strain I71. Members of the genus *Bradyrhizobium* are well-known diazotrophs; additionally, *S. acetylenivorans* SFB93^T was shown to be capable of both acetylenotrophy and diazotrophy (23). Thus, the diazotrophic potential of strain I71 was evaluated. Acetylene was added to the headspace of I71 cells (washed cells in liquid medium) as a carbon and energy source and to be a competitive inhibitor of nitrogenase if expressed (49, 50). Without a bioavailable nitrogen source, cells expressing nitrogenase will reduce nitrogen to ammonium and acetylene to ethylene. Washed and concentrated cells of strain I71 were incubated with and without ammonium and consumed acetylene over time coupled to growth, again confirming their acetylenotrophic metabolism (Fig. 4). Both ammonium-free treatments accumulated ethylene (Fig. 4B), indicating nitrogenase expression in the absence of a bioavailable N source but only after several pulsed additions of acetylene. Higher acetylene concentrations may have been required before observing ethylene accumulation as nitrogen fixation requires a great deal of energy. Trace amounts of surplus bioavailable nitrogen in the cells after washing may also explain the delay in ethylene production. The treatment with additional vitamins and trace elements had higher nitrogenase activity as evidenced by greater ethylene accumulation (Fig. 4B). The rate of ethylene production was higher in cultures with additional vitamins and trace elements (2,066 nmol ethylene hour^{-1} bottle^{-1}) compared to the treatments without amendment (836.7 nmol ethylene hour^{-1} bottle^{-1}). Therefore, ethylene production was not observed in the presence of a readily bioavailable nitrogen source, indicating that nitrogen fixation only occurred in the absence of ammonium. Rates of ethylene production were higher for strain I71 than those observed for *Bradyrhizobium* sp. strains TM122 and TM124 (0.647

TABLE 1 Characteristics of *Bradyrhizobium* strain I71 and related genomes used in this study

Organism	Genome accession no.	Genome size (Mb)	No. of contigs	GC content (%)	Strain-specific gene clusters
Bradyrhizobium sp. I71	PRJNA549647	7.83	1	62.2	522
Bradyrhizobium sp. KBS0725	GCA_005937905.2	7.31	1	62.7	1162
Bradyrhizobium sp. LTSP885	GCA_000938305.1	7.85	43	63.4	1075
Bradyrhizobium sp. UFLA03 84	GCF_002289535.1	8.63	21	64.1	1024
Bradyrhizobium sp. WSM1417	GCA_000515415.1	8.05	1	63.2	765
Bradyrhizobium sp. Yh1	GCA_004346395.1	8.05	41	64.1	655
B. icense LMTR 13	GCA_001693385.1	8.32	1	62.0	1642
B. ottawaense OO99	CP029425	8.61	1	63.8	475
B. zhanjiangense CCBAU 51778	GCA_004114935.1	9.34	1	62.9	1136
Bradyrhizobium sp. URHA0013	GCA_000518345.1	7.19	23	63.8	499
B. japonicum USDA 110	GCA_000011365.1	9.11	1	64.1	286
B. diazoefficiens USDA 122	GCA_001908315.1	9.14	1	64.0	335
B. japonicum USDA 6	GCA_000284375.1	9.21	1	63.7	890
B. elkanii USDA 76^T	GCA_000379145.1	9.48	2	63.7	1059
B. liaoningense CCNWSX0360	GCA_001595995.1	8.59	242	63.7	1092

and 7.81 nmol ethylene hour^{-1} culture^{-1}, respectively) under free-living, oxic conditions (51). In contrast, the rate of ethylene production by strain I71 was lower compared to *Bradyrhizobium* sp. strain DOA9, which was also grown under free-living, oxic conditions (3,644 nmol ethylene hour^{-1} culture^{-1} [52]). Strains TM122, TM124, and DOA9 were initially isolated from plant roots and tested for nitrogen fixation in semisolid media amended with complex carbon substrates to support growth (51, 52). Based on these observations, strain I71 is unique among other free-living *Bradyrhizobium* strains as nitrogen fixation is more typically associated with nodule forming symbiotic *Bradyrhizobium* (53). These results confirm that isolate I71 can transform acetylene via two biochemical pathways, a putative AH and nitrogenase, which has only been demonstrated for the anaerobic acetylenotroph, *S. acetylenivorans* SFB93^T (23).

***Bradyrhizobium* sp. strain I71 genome features.** The *Bradyrhizobium* sp. I71 data set assembled into a single, circular contig of 7,832,041 bp. We annotated 7,392 genes and 7,337 coding sequences, including three rRNA's, 48 tRNA's, and three ncRNA's. Strain I71 contains 522 unique genes that were not identified in the genomes of 14 closely related *Bradyrhizobium* strains as ascertained using Anvi'o (Table 1). These unique genes included a putative AH gene, as discussed below, and several phages and horizontal gene transfer (HGT)-associated genes. HGT has been previously reported in *Bradyrhizobium* in relation to its nitrogen-fixing and root nodulation capabilities (54). Using GhostKOALA KEGG Mapper, we found that the largest class of genes on the I71 genome were involved in genetic information processing (16.0%), followed by environmental information processing (15.2%), signaling and cellular processes (11.9%), carbohydrate metabolism (10.2%), unclassified metabolism (9.6%), amino acid metabolism (8.3%), cellular processes (7.1%), energy metabolism (5%), metabolism of cofactors and vitamins (4%), and other metabolic processes. Of these pathways, 9 complete pathway modules were found for amino acid metabolism indicating that I71 has the genetic potential to metabolize various amino acids, including branched-chain and aromatic amino acids (Table S2). Strain I71 has complete pathway modules for 2 carbohydrate metabolic modules, including glycolysis via the Embden-Meyerhof pathway and carbon metabolism via the tricarboxylic acid (TCA) cycle. Four complete energy metabolism pathway modules were identified, including carbon fixation via the Calvin Cycle (module no. M00165) and phosphate acetyltransferase-acetate kinase pathway (module no. M00579), nitrogen fixation (module no. M00175), denitrification (module no. M00529), and sulfur oxidation (module no. M00595) (Table S2). The presence of nitrogen fixation and carbohydrate metabolism genes is consistent with the metabolism seen in cultures of I71. The nitrogen fixation module was comprised of the proposed minimal gene set (55) for a functional FeMo-nitrogenase (*nif*HDKENB) which was found along with several other nitrogenase-associated genes in the I71 genome (Table S2 and S3). Essential genes for nitrogen fixation were identified in several of the other *Bradyrhizobium* genomes (Table S3) as it is a common phenotype within the genus

(56). Genes used in the conversion of acetyl-CoA to acetate (module no. M00579) are also used in the acetylenotrophic growth of *Syntrophotalea* to gain carbon for cell growth (16).

Other complete pathway modules identified were for lipid metabolism, nucleotide metabolism, signature modules (gene sets that characterize phenotypic features), glycan metabolism, and the metabolism of cofactors and vitamins (Table S2). The genome of I71 contains a complete ModABC molybdate transport system with homologues to *ModA*, *ModB*, and *ModC* detected at locus tags FJV43_07180, FJV43_07185, and FJV43_07190, respectively. No complete tungstate transport system was found, although homologues to *TupA* and *TupB* were detected in the genome. A molybdate transport system and the absence of tungstate transporters is not surprising given that strain I71 was isolated only in the presence of Mo as a cofactor. Given the lack of a complete tungstate pathway in the genome is it unlikely that the strain could also use tungsten as a cofactor for AH.

Although I71 is closely related to known root nodule-forming *Bradyrhizobium*, only the gene for nodulation efficiency protein D (*NfeD*) was identified in its genome. While it is unclear what genes are obligatory for nodulation, genes required for nodule formation by *Bradyrhizobium* are frequently found on a symbiosis island with genes for nitrogen fixation (57). In contrast to the other analyzed *Bradyrhizobium* genomes, no symbiosis islands, plasmid sequences, or other nodulation (*nod*) genes were found in I71.

Identification of a putative AH gene in *Bradyrhizobium* sp. I71. Genome annotation and BLAST searches showed that the I71 genome did not contain any genes with high sequence similarity to the AH from *S. acetylenica* DSM 3246^T, indicating the need for alternative computation approaches to identify a putative AH. Using a hidden Markov model (HMM), we identified a strong, putative AH candidate (locus tag FJV43_01770; interval 384,426 to 386,711, Table S2). The HMM model developed by Gushgari-Doyle et al. (35) showed that this putative AH gene had significant similarity to the known AH genes (score = 506.0, cutoff score = 385.0; E value = 6.1×10^{-152}, cutoff E value = 1.9×10^{-113}).

We used I-TASSER protein prediction software (58, 59) to identify our putative AH candidate's potential structural and functional analogs. The AH of *S. acetylenica* (2e7z; accession no. AF518725.1) was the highest ranked Protein Data Bank (PDB) alignment for all output categories (e.g., structural analog and predicted function) produced by I-TASSER and the second highest ranked template for Gene Ontology (GO) homology (Table S4). This putative AH gene FJV43_01770 was 43.4% identical to the AH reference sequence from *S. acetylenica* (2e7z; accession no. AF518725.1) at the amino acid level (Fig. S7). However, the putative AH FJV43_01770 did not significantly match any gene products in *Bradyrhizobium* isolates with available genome sequences using BLASTn and BLASTp algorithms (Table S2) (60). This might indicate that strain I71 has unique acetylenotrophic capabilities or that other acetylenotrophic *Bradyrhizobium* strains have not been sequenced or discovered to date.

The BLASTp search showed that the putative AH gene had high identities to molybdopterin-dependent oxidoreductases within the molybdopterin-binding (MopB) superfamily of proteins. The top BLASTp hits were a molybdopterin-dependent oxidoreductase from *Nevskia soli* (accession no. WP_051749124; 63.5% sequence identity); dehydrogenase from a *Hyphomicrobiales* freshwater metagenome (accession no. RTL80499; 88.6% identity), and a molybdopterin-dependent oxidoreductase from *Rhodococcus opacus* (accession no. WP_120661552; 61.9% sequence identity). All three of top hits contain a molybdopterin-binding acetylene hydratase C-terminal (cd02781) region, which were computationally predicted based on a separate HMM model (NCBI HMM accession no. NF012602.2). To further elucidate whether the strong putative AH gene from strain I71 (locus tag FJV43_01770) is indeed an AH, we built a protein phylogenetic tree of known and computationally predicted AH containing molybdopterin-binding acetylene hydratase (cd02759) and/or molybdopterin-binding acetylene hydratase C-terminal (cd02781) regions. Interestingly, when performing an "acetylene hydratase" keyword search on the NCBI database, we found over 13,000 hits, which is five times higher than when an identical search was performed in 2018 (16). This, along with the new acetylenotroph presented

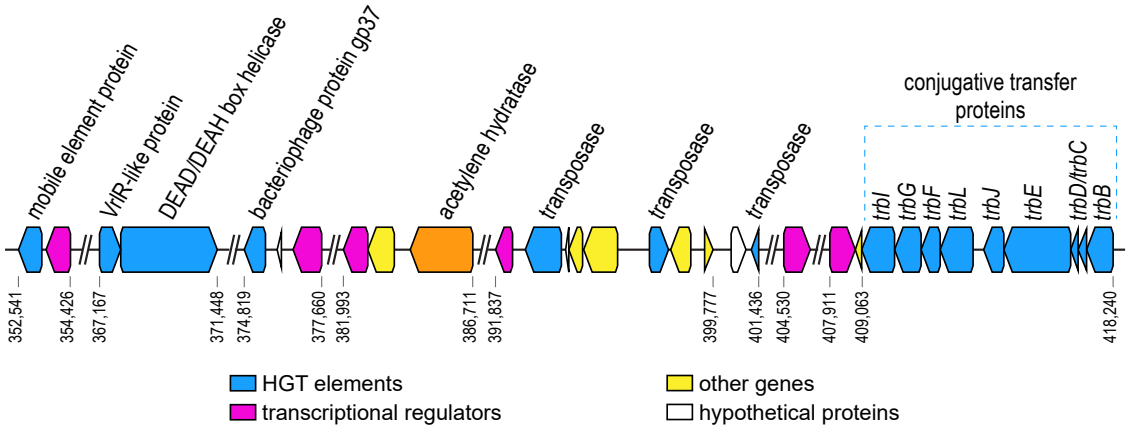

FIG 5 Map of the genomic region flanking the putative acetylene hydratase (AH) gene in *Bradyrhizobium* sp. I71. Double slashes indicate regions of the genome that are omitted for clarity to show the presence of horizontal gene transfer (HGT) elements and transcriptional regulators flanking the putative AH in I71.

here, supports earlier hypotheses that acetylenotrophy may be a ubiquitous metabolic pathway. The known and predicted AH protein sequences clustered separately from other molybdopterin oxidoreductases similar to previous observations (16, 35) (Fig. S8). The strong putative AH gene from strain I71 clustered with sequences from *R. opacus*, *N. soli*, and the metagenome of an acetylenotrophic dechlorinating enrichment culture. These sequences were most closely related to the known AH of acetylenotrophic *Syntrophotalea* species, which was supported by bootstrap values of 100% (Fig. S8). The putative AH sequences computationally predicted by two separate HMM models were similar, and no separate branching was observed based on the model used, providing support for the accuracy of both computational methods. The observation of the strong putative AH clustering with known AH from *Syntrophotalea* species provides support for this being the gene encoding AH. However, additional expression studies are needed for confirmation.

Within 30 kbp of the strong putative AH candidate FJV43_01770 are several genes associated with HGT (Fig. 5). These genes include conjugative transfer proteins, transposases, and viral-like proteins. Similar HGT-implicated genes also flank the AH regions of the acetylenotrophic *Syntrophotalea* (23). It has been hypothesized that AH genes may move via HGT and be associated with the wide phylogenetic diversity of acetylenotrophy across the tree of life (16). While I71 does not contain the same mobile elements found in *S. acetylenivorans* SFB93^T or *S. acetylenica* DSM 3246^T and DSM 3247, it is worth noting the presence of HGT genes colocalized with the putative AH of I71 (Fig. 5).

Twelve molybdopterin oxidoreductases were annotated in the I71 genome using PGAP, but I-TASSER analysis did not strongly predict that any of these sequences could yield an AH. For one molybdopterin oxidoreductase sequence (locus tag FJV43_29500; interval 6,199,194 to 6,201,323), the I-TASSER structure assembly simulation did not include the AH of *S. acetylenica* within the top 10 possible structural analogs. Since the *S. acetylenica* AH reference sequence was not among the top hits, we did not consider it as a strong candidate. Interestingly, the genomes of *Bradyrhizobium ottawaense* OO99 and *Bradyrhizobium zhanjiangense* CCBAU 51778 contained genes with homology to the weakly supported putative AH of I71 (locus tag FJV43_29500; interval 6,199,194 to 6,201,323) based on a BLASTn search. Pairwise alignments between the weakly supported putative AH (locus tag FJV43_29500; interval 6,199,194 to 6,201,323) and the reference sequence from *S. acetylenica* showed just 24.6% identity at the amino acid level. These two strains and 5 other strains of *Bradyrhizobium* were tested for their ability to consume acetylene (Table S3). None of the other *Bradyrhizobium* isolates were shown to consume acetylene with or without the presence of a heterotrophic carbon substrate.

IMPLICATIONS

Members of the *Bradyrhizobium* genus are well known for their agricultural and economic importance due to their ability to improve crop yields via nodule formation and nitrogen fixation (56). Here, we show that this well-known genus also contains a strain (isolate I71) capable of acetylenotrophy, previously undocumented in the *Proteobacteria* phylum. The isolation of *Bradyrhizobium* sp. strain I71 expands the known distribution of acetylenotrophs into the class *Alphaproteobacteria*, confirming our hypothesis that this metabolic pathway is more widespread than previously thought (16). Strain I71 is capable of acetylenotrophy and diazotrophy. The coexistence of these pathways has only been documented in *S. acetylenivorans* SFB93^T (23, 48). Acetylenotrophic activity in a key diazotrophic organism begs the question of why these two pathways would coexist and what selective pressures exist in nature for the maintenance of acetylene metabolism. This is further confounded by the presence of HGT elements flanking the putative AH in strain I71 and the confirmed AH in *Syntrophotalea* strains (23). Acetylenotrophy may be broadly selected based on unknown environmental sources of acetylene or acetylenic compounds (16). As members of the *Bradyrhizobium* are often plant associated, acetylenic plant metabolites could provide a selective substrate for acetylenotrophy. In the case of I71, selection could be primarily driven by soil TCE-contamination as mineral-TCE reactions produce acetylene (29–32). Acetylenotrophy was shown to fuel reductive dechlorination for TCE biodegradation in pure culture consortia (34) and contaminated groundwater (35). These studies showed that anaerobic acetylenotrophs can remove inhibition and generate needed electron donor (H_2) and carbon sources (acetate) for dehalogenating organisms. The presence of aerobic acetylenotrophs in TCE-contaminated soils highlights the potential for *Bradyrhizobium* sp., or other acetylenotrophs, to aid in bioremediation of chlorinated solvents. Based on genome, cultivation, and protein-prediction analysis, acetylenotrophy is likely not widespread within *Bradyrhizobium*, providing more support for TCE-contaminated soils as an environment selective for acetylenotrophy.

MATERIALS AND METHODS

Isolation of an aerobic acetylenotroph. Surface soil was collected from the NASA Ames Research Center on 12 July 2017 under a stand of poplar trees treated for TCE-phytoremediation with an endophytic bacterium (36, 37). Soils were brought to the USGS Menlo Park microbiology lab, air dried, sieved to 2 mm, and stored in a 3.7-L mason jar at room temperature until selective culturing for acetylenotrophic metabolism. Three months after collection, a 200-g subsample of soil was primed with acetylene and then used to construct soil microcosms as described in the supplemental material. Acetylene uptake was measured over time using gas chromatography (GC) with a flame ionization detector (FID) as described in Miller et al. (33). As acetylene concentrations decreased to below detection (<2 μmol/L), the headspace was flushed with sterile air and additional acetylene added to ensure aerobic conditions and availability of acetylene as the primary carbon source. Acetylene was generated from calcium carbide as described in Gushgari-Doyle et al. (35).

The acetylene-consuming microcosms were selected for further enrichment cultivation and isolation using a MOPS-buffered (pH 7.2) mineral medium known as WBMMpAc in the USGS RML. WBMMpAc medium contained (per L): 1.0 g NaCl, 0.4 g $MgCl_2$*$6H_2O$, 0.1 g $CaCl_2$*H_2O, 0.5 g KCl, 0.3 g NH_4Cl, 0.6 g KH_2PO_4, 5.0 g MOPS (3-morpholinopropane-1-sulfonic acid), 1 mL of trace element solution (TES) SL9 (61), and 1 mL vitamin solution M141 (Vit-M141) (62). The detailed media recipe is provided in the supplemental material. The medium was filter-sterilized using a Corning bottle top filtration unit containing a 0.22 μm polyethersulfone (PES) membrane (Corning, Inc., Corning, New York). This medium was dispensed aseptically into serum bottles and sealed with sterile butyl rubber stoppers (Bellco) and aluminum crimp seals. All media preparation was performed in a class II, type B2 Laminar Flow Biological Safety Cabinet (NuAire, Inc., Plymouth, Minnesota). The medium was inoculated with 1 mL of microcosm soil slurry. Then, the air headspace was amended with 1% acetylene by volume and sterile air was added to reach an overpressure of ~30,000 Pa. Headspace pressure was measured using a GMH 3111 digital pressure meter with a GMSD needle pressure transducer (Greisinger Electronic, Germany). The cultures were incubated at room temperature in the dark without shaking. Acetylene consumption was monitored by GC using a thermal conductivity detector (TCD) or FID as described in the supplemental material.

A stable acetylenotrophic enrichment culture was obtained from a single microcosm replicate. The culture was transferred twice to verify acetylenotrophic activity and used for isolation via a combination of agar shakes, serial dilutions, and plate bottle methods. Agar shakes were a soft agar medium that was inoculated prior to solidification to separate cells in the medium matrix. To construct the agar shakes, we combined an autoclaved solution of 8% agar with filter-sterilized WBMMpAc medium to yield a 0.8% final concentration of agar. The medium was inoculated at a temperature of ~50°C, swirled to mix, then

solidified in an ice bath. Agar shake cultures were incubated at room temperature in the dark. A single colony was picked from the agar shake using a sterile glass Pasteur pipet to inoculate a new round of liquid WBMMpAc medium cultures. This step was used to verify that the organisms were using acetylene as their primary carbon source and not carbon substrates from the agarose. Once the liquid culture grew (growth determined by visual observations of turbidity) and acetylene consumption was observed, the liquid culture was used for a second round of agar shakes (which resulted in 3 colonies), followed by liquid medium cultivation. Picking isolated colonies from agar shakes proved challenging, therefore the 3 liquid cultures were subsequently used for serial dilutions to isolate an acetylenotrophic organism. The liquid cultures were serially diluted 10^{-1} to 10^{-10} in liquid WBMMpAc medium and incubated at room temperature in the dark. Growth and acetylene consumption were measured over time and the highest positive dilutions showing acetylenotrophic activity were used for isolation using a plate bottle technique.

Plate bottles were designed as an alternative to petri plates, as isolation of the acetylenotroph required a controlled headspace where acetylene gas could be added as a substrate (and measured for activity) while allowing separation of individual cells. To construct plate bottles, we combined an autoclaved solution of 3% agar with filter-sterilized WBMMpAc medium to yield a 1.5% final concentration of agar in a 250-mL Schott bottle. Bottles were capped then laid on an angle (see Fig. S1) while the media solidified overnight to provide a greater surface area. After solidification, the bottles had condensation and were subsequently dried uncapped on their side for 2 to 3 h in a biological safety cabinet. The solid media surface was inoculated using a loop, then the bottles were capped with sterile GL45 butyl rubber stoppers and aperture caps (Ochs GmbH, Germany). The headspace was overpressured with sterile air and amended with C_2H_2. The bottles were incubated upside-down to avoid condensation on the agarose surface. Acetylene was measured over time by GC-TCD, and colonies were transferred by streak plating three times to ensure purity.

The resulting isolate, strain I71, was transferred and maintained in WBMMpAc liquid medium in the USGS RML (Fig. S2). Biomass was collected and used for determining the phylogenetic identity of the isolate I71 based on 16S rRNA gene sequencing as described in the supplemental methods. I71 was also capable of heterotrophic growth in LMG135, which contained yeast extract and mannitol (63), and in modified arabinose gluconate medium (MAG, ATCC medium 2233). A culture of I71 in MAG medium was submitted to the German Collection of Microorganisms and Cell Cultures (DSMZ) and deposited under accession number DSM 112639.

Acetylenotrophic and heterotrophic growth assays. To demonstrate growth coupled to acetylenotrophic and heterotrophic activity, we conducted assays with 2 cell lines of I71 ("RML_I71" or "DSMZ_I71"). Experiments were performed with both cell lines to confirm that consistent results could be obtained when starting with different cultures. "RML_I71" is the cell line maintained in acetylenotrophic media at the USGS RML. "DSMZ_I71" is the culture received from the DSMZ for the depositor check; the culture was revived from the lyophilized culture in MAG media, transferred once in MAG, then used as inoculum directly into WBMMpAc medium for growth assays.

For the growth studies, WBMMpAc liquid medium was prepared as described above then dispensed aseptically into 100 mL serum bottles and sealed with sterile butyl rubber stoppers (Bellco) and aluminum crimp seals. Bottles were set up for the following treatments: (i) + acetylene (sole carbon source provided); (ii) no carbon source; (iii) + acetylene and yeast extract; and (iv) + yeast extract. For treatments i and ii, bottles received 50 mL of liquid media, while treatments iii and iv had 40 mL of liquid medium due to limited volumes of media available at the start of the experiment. Acetylene (1 mL) was added to bottles for treatments i and iii, while bottles for treatments iii and iv received 0.5 mL of 10% yeast extract. The air headspace of all bottles was overpressured with sterile air. Triplicate bottles for each treatment were inoculated with 0.25 mL inoculum from either the RML_I71 or DSMZ_I71 cell lines or left uninoculated as a medium control. Bottles were incubated at 30°C in the dark without shaking.

Optical density (OD_{600}) was measured on each bottle using a GENESYS 6 UV-Vis spectrophotometer (Thermo Fisher Scientific) with thorough vortexing prior to each OD_{600} measurement. Acetylene concentrations were measured in the headspace of treatments i and iii using GC-FID as described in the supplemental methods. Aqueous samples were collected for cell counts at the beginning of the experiment, after a significant change in OD_{600}, and once most of the acetylene was consumed. Cell count samples were preserved in 1% glutaraldehyde (final concentration) and frozen at −80°C until determination of cell densities by acridine orange direct cell counts (64).

Nitrogen fixation assays. Strain I71 was grown in 500 mL of WBMMpAc liquid media to late log-phase with acetylene as the sole carbon substrate (as described above). Late log-phase cells were harvested by centrifugation (5,000 × *g* for 30 min). Pelleted cells were washed 3 times by resuspending in 30 mL of WBMMpAc basal salts without trace elements, vitamins, or ammonium followed by centrifugation (5,000 × *g* for 30 min) and then brought back to 50 mL volume. Cell suspensions were dispensed (5 mL) into Balch tubes and sealed with an air headspace. Triplicate cultures were set up with the following treatment conditions: (i) no amendment (incubation in ammonium-free media), (ii) ammonium-free media with modified TES-SL10 and modified Wolin vitamin solution, or (iii) amended with NH_4Cl to a final concentration of 0.6 mM NH_4Cl. TES-SL10 was used for nitrogen fixation assays to omit all dinitrogen sources; recipes for modified TES-SL10 and Wolin vitamins are provided in the supplemental material. All cultures were amended with 1 mL of C_2H_2 as the sole carbon source (total of 5 pulses over time) and incubated in the dark at 28°C. Headspace analyses of C_2H_2 and C_2H_4 were carried out GC-FID as described previously (33). Henry's Law K_H values employed were 4×10^{-2} for C_2H_2 and 4.8×10^{-3} for C_2H_4, as calculated previously in Miller et al. (65). Growth was determined spectrophotometrically by OD_{600}.

Genome sequencing, assembly, and annotation. The isolate was grown to high density in mannitol yeast extract medium (LMG 135; [63]) at room temperature while shaking at 100 rpm. Biomass was

pelleted by centrifugation (5,000 × *g* for 15 min) then frozen at −20°C until DNA extraction. Genomic DNA was extracted from cell pellets utilizing a phenol-chloroform extraction method modified from (66). DNA concentrations and purity were measured with a Qubit 4 (Life Technologies, Carlsbad, CA, USA) and NanoDrop 1000 spectrophotometer (Thermo Fischer Scientific, Waltham, MA, USA), respectively. Extracts were visualized on a 0.8% agarose gel to verify recovery of high molecular weight gDNA.

Genome sequencing was carried out using Oxford Nanopore Technologies (ONT) and Illumina platforms to generate long- and short-read data sets, respectively. One microgram of gDNA was prepared for multiplex sequencing by attaching unique barcodes from the ONT native barcoding kit (EXP-NBD104). Following barcoding, the sample was pooled in equimolar amounts and further prepared for sequencing using the ONT ligation sequencing kit (SQK-LSK109). The multiplexed library was sequenced on an R9.4.1 flow cell using a GridION X5 platform. The sequence data were demultiplexed and trimmed of adapters and barcode sequences using Porechop (https://github.com/rrwick/Porechop). Aliquots of gDNA were sent to the Microbial Genome Sequencing Center (MiGS, Pittsburgh, PA, USA) for 150 bp paired-end sequencing. The sample was prepared for sequencing using an Illumina Nextera kit (Illumina Inc. San Diego, CA, USA) and sequenced on an Illumina NextSeq 550 platform. Hybrid genome assemblies were generated using both ONT long reads and 150 bp reads using MaSuRCA v.3.3.4 (67). Following polishing with Pilon (68), gene annotation was performed using the Prokaryotic Genome Annotation Pipeline (PGAP) from NCBI (69). To identify functional pathways, the I71 genome was also annotated using eggNOG-mapper (70, 71) to generate a list of Kyoto Encyclopedia of Genes and Genomes (KEGG) (72) orthologs (KOs) which were then mapped to pathways using GhostKOALA (73).

***Bradyrhizobium* genome comparisons.** The assembled and annotated sequences from I71 were compared using average nucleotide identity (ANI) (74) to determine their similarity. To determine where the I71 isolate fell within the genus *Bradyrhizobium*, the program Up-to-Date Bacterial Core Genome (UBCG) (75) was used to annotate, extract, and align 92 genes from *Bradyrhizobium* genomes and the genome of *Oligotropha carboxidovorans* was used as an outgroup. The 92 alignments were concatenated in Geneious Prime v.2019.2.3 (76), and the phylogeny was inferred using IQ-TREE (77, 78). IQ-TREE was run using the standard model selection option, and branch supports were obtained based on 1,000 bootstrap replicates with the ultrafast bootstrap (79) algorithm implemented in the IQ-TREE software (77, 78).

Genomes from 14 other *Bradyrhizobium* were identified and downloaded from the National Center of Biotechnology Information (NCBI) (80) and the Joint Genome Institute (81) for comparison of gene content within members of the genus *Bradyrhizobium*. Genomic comparisons for these genomes were made using the Anvi'o 6.2 (82) workflow described by Delmont and Eren (83). Contig databases for the comparative analysis were created using the command anvi-gen-contigs-database and then further refined using hmm-scan and anvi-run-ncbi-cog. The pangenome was then created using anvi-pan-genome with the parameters "--minbit 0.5," "--mcl-inflation 6," and "--use-ncbi-blast." Once Anvi'o created the pangenome output, all singleton genes were binned into a single collection within Anvi'o using a parameter search. A list of all gene clusters was created using "generate static html summary" where the gene clusters were trimmed to include only singleton genes from I71. A subset of the selected *Bradyrhizobium* genomes were analyzed using OrthoANI (84) to determine pairwise identities. BLASTn (60) and BLASTp searches were used to investigate the presence or absence of genes in the I71 genome with high sequence similarity to the *ahy* gene from *S. acetylenica* DSM 3246^T (formerly *Pelobacter acetylenicus* [17]).

Identification of putative acetylene hydratase (AH). Putative AH genes in the I71 genome were identified using two approaches. First, all PGAP annotated molybdopterin oxidoreductases were extracted from the genome using Geneious Prime v.2019.2.3. Then, sequences were entered into I-TASSER (58, 59, 85) to determine the likelihood that the genes could code for AH. I-TASSER is a protein structure and function prediction program that operates via a threading algorithm to predict a protein's 3-D structural model from amino acid sequences in comparison to templates from the Protein Data Bank (PDB). A putative AH was considered a strong candidate when the I-TASSER results had the AH from *S. acetylenica* DSM 3246^T as the top hit in all categories. The sequence was considered a weak candidate if the *S. acetylenica* AH was not the top hit in all categories but still was considered a possible match by I-TASSER. The second approach employed an HMM model, developed by Gushgari-Doyle et al. (35), to specifically identify putative AH genes from sequence data. The HMM model was run on the amino acid sequences of all genes annotated by PGAP. As described above, sequences identified with the HMM model were then tested using I-TASSER. Candidate putative AH sequences were compared to AH sequences from the genome of *S. acetylenica* DSM 3246^T and *S. acetylenivorans* SFB93^T (86, 87), reference sequences from the NCBI database (88), and metagenome-derived putative AH from acetylene-fueled dechlorinating enrichment cultures (35). Amino acid sequences were aligned using Muscle 3.8.425 (89) prior to tree reconstruction using FastTree v.2.1.11 (90) in Geneious Prime v.2022.1 (76). Default FastTree approximately maximum-likelihood parameters were used, and support values were based on 1,000 resamples.

Acetylenotrophy assays with other *Bradyrhizobium* species. Seven additional *Bradyrhizobium* isolates were tested for acetylenotrophic activity in parallel with *Bradyrhizobium* sp. I71 (Table S2). Cultures of *B. ottawaense* OO99 and *B. zhanjiangense* CCBAU 51778 were obtained from the Belgian Coordinated Collections of Microorganisms. *Bradyrhizobium* sp. URHA0013 was provided by Eoin Brodie, Lawrence Berkeley National Laboratory. Cultures of *B. japonicum* USDA 110^T and USDA 6^T and *Bradyrhizobium elkanii* USDA 76^T were provided by Patrick Elia, U.S. Department of Agriculture. *Bradyrhizobium diazoeffeciens* USDA 122 was provided by Jeffry Fuhrmann, University of Delaware. Cultures were grown on modified arabinose gluconate medium (MAG, ATCC medium 2233) then streaked onto MAG solid medium and grown at 28°C to obtain distinct colonies. To test acetylenotrophic activity, colonies were transferred to WBMMpAc media in sealed Balch tubes prepared as described above with an oxic, acetylene-containing headspace. *Bradyrhizobium* sp. strain I71 was also grown on MAG plates then transferred to WBMMpAc

as a positive control. Cultures were incubated at 28°C in the dark. Headspace analysis of C_2H_2 and O_2 were performed using gas chromatography, as described above, and growth was measured spectrophotometrically by OD_{600}. After 3 to 4 weeks, no acetylenotrophic activity was observed, so the cultures were amended with dilute yeast extract as an attempt to stimulate acetylene consumption with heterotrophic growth as required by some *Actinobacteria* acetylenotrophs (28).

Data availability. Illumina 16S iTag sequence data for the microcosms were deposited in GenBank under BioProject number PRJNA701273. The 16S rRNA gene sequence from Sanger sequencing was deposited in GenBank under the accession number MW587253. The genome of isolate I71 was deposited in GenBank under BioProject PRJNA549647 (genome accession number CP059398; BioSample SAMN12094990). Strain I71 was deposited in the German Collection of Microorganisms and Cell Cultures (DSMZ) under accession number DSM 112639. Data for acetylenotrophic, heterotrophic, and diazotrophic experiments are available from Baesman et al. (38).

SUPPLEMENTAL MATERIAL

Supplemental material is available online only.

SUPPLEMENTAL FILE 1, PDF file, 2.8 MB.

SUPPLEMENTAL FILE 2, XLSX file, 0.05 MB.

ACKNOWLEDGMENTS

We thank M. Mihori, C. Harris, B. Polite, P. Bouwma, and J. Switzer Blum for laboratory and bioinformatic assistance. In addition, we thank Jeff Fuhrmann and Prasanna Joglekar (University of Delaware); Dave Westenberg (Missouri University of Science and Technology); Patrick Elia (U.S. Department of Agriculture); and Eoin Brodie, Patrick Sorensen, and Shi Wang (Lawrence Berkeley National Laboratory) for providing *Bradyrhizobium* strains for testing. We also thank Prasanna Joglekar (University of Delaware), Dwayne Elias (Oak Ridge National Lab), and Michael Wells (Oak Ridge National Lab) for helpful discussions.

This work was supported by a NASA Research Opportunities in Space and Earth Science (ROSES-2013), Astrobiology: Exobiology and Evolutionary Biology Program Element grant (grant 13-EXO13-0001) to D.M.A. and R.S.O. Funding was also provided by the U.S. Geological Survey Environmental Health Program (Toxic Substances Hydrology and Contaminant Biology) and the Water Mission Area. In addition, J.M.S. and J.L.F. were supported by NSF uRoL 1921585 and NSF DEB 1941854.

Any use of trade, firm, or product names is for descriptive purposes only and does not imply endorsement by the U.S. Government. We declare no competing financial interest.

Conceptualization, J.M.S., R.S.O., J.L.F., and D.M.A.; Methodology, J.M.S., S.M.B., Y.S., R.A., S.G.-D., M.K., J.L.F., and D.M.A.; Investigation, J.M.S., T.J.B., S.M.B., E.K., Y.S., R.A., M.K., J.L.F., S.G.-D., and D.M.A.; Writing – Original Draft, J.M.S., T.J.B., J.L.F., S.M.B., R.S.O., M.K., and D.M.A.; Writing – Review & Editing, D.M.A., J.L.F., and S.M.B.; Visualization, J.M.S., T.J.B., S.M.B., and D.M.A.; Funding Acquisition, J.L.F., R.S.O., and D.M.A.

REFERENCES

1. Cronn D, Robinson E. 1979. Tropospheric and lower stratospheric vertical profiles of ethane and acetylene. Geophys Res Lett 6:641–644. https://doi.org/10.1029/GL006i008p00641.
2. Goldman A, Murcray FJ, Blatherwick RD, Gillis JR, Bonomo FS, Murcray FH, Murcray DG, Cicerone RJ. 1981. Identification of acetylene (C_2H_2) in infrared atmospheric absorbtion spectra. J Geophys Res 86:12143–12146. https://doi.org/10.1029/JC086iC12p12143.
3. Rudolph J, Ehhalt DH, Khedim A. 1984. Vertical profiles of acetylene in the troposphere and stratosphere. J Atmos Chem 2:117–124. https://doi.org/10.1007/BF00114125.
4. Arnts RR, Meeks SA. 1981. Biogenic hydrocarbon contribution to the ambient air of selected areas. Atmospheric Environment 15:1643–1651. https://doi.org/10.1016/0004-6981(81)90149-9.
5. Bonsang B, Martin D, Lambert G, Kanakidou M, Le Roulley JC, Sennequier G. 1991. Vertical distribution of non methane hydrocarbons in the remote marine boundary layer. J Geophys Res 96:7313–7324. https://doi.org/10.1029/90JD02539.
6. Cofer WR, Levine JS, Winstead EL, LeBel PJ, Koller AM, Hinkle CR. 1990. Trace gas emissions from burning Florida wetlands. J Geophys Res 95:1865–1870. https://doi.org/10.1029/JD095iD02p01865.
7. Kanakidou M, Bonsang B, Le Roulley JC, Lambert G, Martin D, Sennequier G. 1988. Marine source of atmospheric acetylene. Nature 333:51–52. https://doi.org/10.1038/333051a0.
8. Stewart WD, Fitzgerald GP, Burris RH. 1967. *In situ* studies on N_2 fixation using the acetylene reduction technique. Proc Natl Acad Sci U S A 58:2071–2078. https://doi.org/10.1073/pnas.58.5.2071.
9. Yoshinari T, Hynes R, Knowles R. 1977. Acetylene inhibition of nitrous oxide reduction and measurement of denitrification and nitrogen fixation in soil. Soil Biol Biochem 9:177–183. https://doi.org/10.1016/0038-0717(77)90072-4.
10. Hynes RK, Knowles R. 1978. Inhibition by acetylene of ammonia oxidation in *Nitrosomonas europaea*. FEMS Microbiology Lett 4:319–321. https://doi.org/10.1111/j.1574-6968.1978.tb02889.x.
11. Oremland RS, Taylor BF. 1975. Inhibition of methanogenesis in marine sediments by acetylene and ethylene: validity of the acetylene reduction assay for anaerobic microcosms. Appl Microbiol 30:707–709. https://doi.org/10.1128/am.30.4.707-709.1975.
12. Colby J, Dalton H. 1976. Some properties of a soluble methane monooxygenase from *Methylococcus capsulatus* strain Bath. Biochem J 157:495–497. https://doi.org/10.1042/bj1570495.
13. Prior SD, Dalton H. 1985. Acetylene as a suicide substrate and active site probe for methane monooxygenase from *Methylococcus capsulatus* (Bath).

FEMS Microbiology Lett 29:105–109. https://doi.org/10.1111/j.1574-6968.1985.tb00843.x.
14. Warren MJ, Lin X, Gaby JC, Kretz CB, Kolton M, Morton PL, Pett-Ridge J, Weston DJ, Schadt CW, Kostka JE, Glass JB. 2017. Molybdenum-based diazotrophy in a *Sphagnum* Peatland in Northern Minnesota. Appl Environ Microbiol 83:e01174-17. https://doi.org/10.1128/AEM.01174-17.
15. Pon G, Hyman MR, Semprini L. 2003. Acetylene inhibition of trichloroethene and vinyl chloride reductive dechlorination. Environ Sci Technol 37:3181–3188. https://doi.org/10.1021/es026352i.
16. Akob DM, Sutton JM, Fierst JL, Haase KB, Baesman S, Luther GW, Miller LG, Oremland RS. 2018. Acetylenotrophy: a hidden but ubiquitous microbial metabolism? FEMS Microbiol Ecol 94:fiy103. https://doi.org/10.1093/femsec/fiy103.
17. Waite DW, Chuvochina M, Pelikan C, Parks DH, Yilmaz P, Wagner M, Loy A, Naganuma T, Nakai R, Whitman WB, Hahn MW, Kuever J, Hugenholtz P. 2020. Proposal to reclassify the proteobacterial classes *Deltaproteobacteria* and *Oligoflexia*, and the phylum *Thermodesulfobacteria* into four phyla reflecting major functional capabilities. Int J Syst Evol Microbiol 70:5972–6016. https://doi.org/10.1099/ijsem.0.004213.
18. Schink B. 1985. Fermentation of acetylene by an obligate anaerobe, *Pelobacter acetylenicus* sp. nov. Arch Microbiol 142:295–301. https://doi.org/10.1007/BF00693407.
19. ten Brink F. 2014. Living on acetylene. A primordial energy source, p 15–35. *In* Kroneck PMH, Torres MES (ed), The Metal-Driven Biogeochemistry of Gaseous Compounds in the Environment, Metal Ions in Life Sciences, 2014/11/25 ed, vol 14. Springer, Dordrecht, Berlin, Germany.
20. Seiffert GB, Ullmann GM, Messerschmidt A, Schink B, Kroneck PM, Einsle O. 2007. Structure of the non-redox-active tungsten/[4Fe:4S] enzyme acetylene hydratase. Proc Natl Acad Sci U S A 104:3073–3077. https://doi.org/10.1073/pnas.0610407104.
21. ten Brink F, Schink B, Kroneck PMH. 2011. Exploring the active site of the tungsten, iron-sulfur enzyme acetylene hydratase. J Bacteriol 193:1229–1236. https://doi.org/10.1128/JB.01057-10.
22. Rosner BM, Schink B. 1995. Purification and characterization of acetylene hydratase of *Pelobacter acetylenicus*, a tungsten iron-sulfur protein. J Bacteriol 177:5767–5772. https://doi.org/10.1128/jb.177.20.5767-5772.1995.
23. Akob DM, Baesman SM, Sutton JM, Fierst JL, Mumford AC, Shrestha Y, Poret-Peterson AT, Bennett S, Dunlap DS, Haase KB, Oremland RS. 2017. Detection of diazotrophy in the acetylene-fermenting anaerobe *Pelobacter* sp. strain SFB93. Appl Environ Microbiol 83:e01198-17. https://doi.org/10.1128/AEM.01198-17.
24. Birch-Hirschfeld L. 1932. Die Umsetzung von Acetylen durch *Mycobacterium lacticola*. Zentralbl Bakteriol Parasitenkd Infektionskr Hyg Abt 86:113–130.
25. de Bont JAM, Peck MW. 1980. Metabolism of acetylene by *Rhodococcus* A1. Arch Microbiol 127:99–104. https://doi.org/10.1007/BF00428012.
26. Kanner D, Bartha R. 1982. Metabolism of acetylene by *Nocardia rhodochrous*. J Bacteriol 150:989–992. https://doi.org/10.1128/jb.150.2.989-992.1982.
27. Germon JC, Knowles R. 1988. Metabolism of acetylene and acetaldehyde by *Rhodococcus rhodochrous*. Can J Microbiol 34:242–248. https://doi.org/10.1139/m88-045.
28. Rosner BM, Rainey FA, Kroppenstedt RM, Schink B. 1997. Acetylene degradation by new isolates of aerobic bacteria and comparison of acetylene hydratase enzymes. FEMS Microbiol Lett 148:175–180. https://doi.org/10.1111/j.1574-6968.1997.tb10285.x.
29. Roberts AL, Totten LA, Arnold WA, Burris DR, Campbell TJ. 1996. Reductive elimination of chlorinated ethylenes by zero-valent metals. Environ Sci Technol 30:2654–2659. https://doi.org/10.1021/es9509644.
30. Arnold WA, Roberts AL. 2000. Pathways and kinetics of chlorinated ethylene and chlorinated acetylene reaction with Fe(0) particles. Environ Sci Technol 34:1794–1805. https://doi.org/10.1021/es990884q.
31. Han YS, Hyun SP, Jeong HY, Hayes KF. 2012. Kinetic study of cis-dichloroethylene (cis-DCE) and vinyl chloride (VC) dechlorination using green rusts formed under varying conditions. Water Res 46:6339–6350. https://doi.org/10.1016/j.watres.2012.08.041.
32. Schaefer CE, Towne RM, Lippincott DR, Lacombe PJ, Bishop ME, Dong H. 2015. Abiotic dechlorination in rock matrices impacted by long-term exposure to TCE. Chemosphere 119:744–749. https://doi.org/10.1016/j.chemosphere.2014.08.005.
33. Miller LG, Baesman SM, Kirshtein J, Voytek MA, Oremland RS. 2013. A biogeochemical and genetic survey of acetylene fermentation by environmental samples and bacterial isolates. Geomicrobiol J 30:501–516. https://doi.org/10.1080/01490451.2012.732662.
34. Mao X, Oremland RS, Liu T, Gushgari S, Landers AA, Baesman SM, Alvarez-Cohen L. 2017. Acetylene fuels TCE reductive dechlorination by defined *Dehalococcoides/Pelobacter* consortia. Environ Sci Technol 51:2366–2372. https://doi.org/10.1021/acs.est.6b05770.
35. Gushgari-Doyle S, Oremland RS, Keren R, Baesman SM, Akob DM, Banfield JF, Alvarez-Cohen L. 2021. Acetylene-fueled trichloroethene reductive dechlorination in a groundwater enrichment culture. mBio 12:e02724-20. https://doi.org/10.1128/mBio.02724-20.
36. Kang JW, Khan Z, Doty SL. 2012. Biodegradation of trichloroethylene by an endophyte of hybrid poplar. Appl Environ Microbiol 78:3504–3507. https://doi.org/10.1128/AEM.06852-11.
37. Doty SL, Freeman JL, Cohu CM, Burken JG, Firrincieli A, Simon A, Khan Z, Isebrands JG, Lukas J, Blaylock MJ. 2017. Enhanced degradation of TCE on a superfund site using endophyte-assisted Poplar tree phytoremediation. Environ Sci Technol 51:10050–10058. https://doi.org/10.1021/acs.est.7b01504.
38. Baesman SM, Klein E, Andrews RS, Shrestha Y, Bushman TJ, Sutton JM, Akob DM. 2022. Data on the enrichment and isolation of the acetylenotrophic and diazotrophic isolate *Bradyrhizobium* sp. strain I71, version 2.0. U.S. Geological Survey data release. https://doi.org/10.5066/P9DUG9O3.
39. Baesman SM, Sutton JM, Fierst JL, Akob DM, Oremland RS. 2019. *Syntrophotalea acetylenivorans* sp. nov., a diazotrophic, acetylenotrophic anaerobe isolated from intertidal sediments. Int J Syst Evol Microbiol 71:e004698. https://doi.org/10.1099/ijsem.0.004698.
40. Sameshima R, Isawa T, Sadowsky MJ, Hamada T, Kasai H, Shutsrirung A, Mitsui H, Minamisawa K. 2003. Phylogeny and distribution of extra-slow-growing *Bradyrhizobium japonicum* harboring high copy numbers of RSa, RSß and IS*1631*. FEMS Microbiol Ecol 44:191–202. https://doi.org/10.1016/S0168-6496(03)00009-6.
41. Avontuur JR, Palmer M, Beukes CW, Chan WY, Coetzee MPA, Blom J, Stępkowski T, Kyrpides NC, Woyke T, Shapiro N, Whitman WB, Venter SN, Steenkamp ET. 2019. Genome-informed *Bradyrhizobium* taxonomy: where to from here? Syst Appl Microbiol 42:427–439. https://doi.org/10.1016/j.syapm.2019.03.006.
42. Joglekar P, Mesa CP, Richards VA, Polson SW, Wommack KE, Fuhrmann JJ. 2020. Polyphasic analysis reveals correlation between phenotypic and genotypic analysis in soybean bradyrhizobia (*Bradyrhizobium* spp.). Syst Appl Microbiol 43:126073. https://doi.org/10.1016/j.syapm.2020.126073.
43. Konstantinidis KT, Rosselló-Móra R, Amann R. 2017. Uncultivated microbes in need of their own taxonomy. ISME J 11:2399–2406. https://doi.org/10.1038/ismej.2017.113.
44. Marcondes de Souza JA, Carareto Alves LM, de Mello Varani A, de Macedo Lemos EG. 2014. The Family *Bradyrhizobiaceae*, p 135–154. *In* Rosenberg E, DeLong EF, Lory S, Stackebrandt E, Thompson F (ed), The Prokaryotes: *alphaproteobacteria* and *Betaproteobacteria*. Springer Berlin Heidelberg, Berlin, Heidelberg. https://doi.org/10.1007/978-3-642-30197-1_253.
45. Kaneko T, Nakamura Y, Sato S, Minamisawa K, Uchiumi T, Sasamoto S, Watanabe A, Idesawa K, Iriguchi M, Kawashima K, Kohara M, Matsumoto M, Shimpo S, Tsuruoka H, Wada T, Yamada M, Tabata S. 2002. Complete genomic sequence of nitrogen-fixing symbiotic bacterium *Bradyrhizobium japonicum* USDA110. DNA Res 9:189–197. https://doi.org/10.1093/dnares/9.6.189.
46. VanInsberghe D, Maas KR, Cardenas E, Strachan CR, Hallam SJ, Mohn WW. 2015. Non-symbiotic *Bradyrhizobium* ecotypes dominate North American forest soils. ISME J 9:2435–2441. https://doi.org/10.1038/ismej.2015.54.
47. So RB, Ladha JK, Young JP. 1994. Photosynthetic symbionts of *Aeschynomene* spp. form a cluster with *Bradyrhizobia* on the basis of fatty acid and rRNA analyses. Int J Syst Bacteriol 44:392–403. https://doi.org/10.1099/00207713-44-3-392.
48. Baesman SM, Sutton JM, Fierst JL, Akob DM, Oremland RS. 2019. *Syntrophotalea acetylenivorans*, strain SFB93, sp. nov., a diazotrophic, acetylenotrophic anaerobe isolated from intertidal sediments. Int J Syst Evol Microbiol in Press 71. https://doi.org/10.1099/ijsem.0.004698.
49. Schöllhorn R, Burris RH. 1967. Acetylene as a competitive inhibitor of N-2 fixation. Proc Natl Acad Sci U S A 58:213–216. https://doi.org/10.1073/pnas.58.1.213.
50. Dilworth MJ. 1966. Acetylene reduction by nitrogen-fixing preparations from *Clostridium pasteurianum*. Biochimica et Biophysica Acta (BBA) - General Subjects 127:285–294. https://doi.org/10.1016/0304-4165(66)90383-7.
51. Hara S, Morikawa T, Wasai S, Kasahara Y, Koshiba T, Yamazaki K, Fujiwara T, Tokunaga T, Minamisawa K. 2019. Identification of nitrogen-fixing *Bradyrhizobium* associated with roots of field-grown sorghum by metagenome and proteome analyses. Front Microbiol 10:407. https://doi.org/10.3389/fmicb.2019.00407.
52. Wongdee J, Boonkerd N, Teaumroong N, Tittabutr P, Giraud E. 2018. Regulation of nitrogen fixation in *Bradyrhizobium* sp. strain DOA9 involves

two distinct NifA regulatory proteins that are functionally redundant during symbiosis but not during free-living growth. Front Microbiol 9:1644. https://doi.org/10.3389/fmicb.2018.01644.
53. Ormeno-Orrillo E, Martinez-Romero E. 2019. A genomotaxonomy view of the *Bradyrhizobium* genus. Front Microbiol 10:1334. https://doi.org/10.3389/fmicb.2019.01334.
54. Barcellos FG, Menna P, da Silva Batista JS, Hungria M. 2007. Evidence of horizontal transfer of symbiotic genes from a *Bradyrhizobium japonicum* inoculant strain to indigenous diazotrophs *Sinorhizobium* (*Ensifer*) *fredii* and *Bradyrhizobium elkanii* in a Brazilian Savannah soil. Appl Environ Microbiol 73:2635–2643. https://doi.org/10.1128/AEM.01823-06.
55. Dos Santos PC, Fang Z, Mason SW, Setubal JC, Dixon R. 2012. Distribution of nitrogen fixation and nitrogenase-like sequences amongst microbial genomes. BMC Genomics 13:162. https://doi.org/10.1186/1471-2164-13-162.
56. Rosenberg E, DeLong EF, Lory S, Stackebrandt E, Thompson F (ed). 2014. The Prokaryotes—Alphaproteobacteria and Betaproteobacteria. Springer-Verlag, Berlin, Heidelberg.
57. Göttfert M, Röthlisberger S, Kündig C, Beck C, Marty R, Hennecke H. 2001. Potential symbiosis-specific genes uncovered by sequencing a 410-kilobase DNA region of the *Bradyrhizobium japonicum* chromosome. J Bacteriol 183:1405–1412. https://doi.org/10.1128/JB.183.4.1405-1412.2001.
58. Yang J, Yan R, Roy A, Xu D, Poisson J, Zhang Y. 2015. The I-TASSER Suite: protein structure and function prediction. Nat Methods 12:7–8. https://doi.org/10.1038/nmeth.3213.
59. Yang J, Zhang Y. 2015. I-TASSER server: new development for protein structure and function predictions. Nucleic Acids Res 43:W174–W181. https://doi.org/10.1093/nar/gkv342.
60. Madden T. 2002. The BLAST sequence analysis tool. *In* McEntyre J, Ostell J (ed), The NCBI Handbook. National Center for Biotechnology Information, Bethesda, Maryland, USA.
61. Tschech A, Pfennig N. 1984. Growth yield increase linked to caffeate reduction in *Acetobacterium woodii*. Arch Microbiol 137:163–167. https://doi.org/10.1007/BF00414460.
62. Zeikus JG, Hegge PW, Thompson TE, Phelps TJ, Langworthy TA. 1983. Isolation and description of *Haloanaerobium praevalens* gen. nov. and sp. nov., an obligately anaerobic halophile common to Great Salt Lake sediments. Curr Microbiol 9:225–233. https://doi.org/10.1007/BF01567586.
63. Atlas RM. 2004. Handbook of microbiological media, vol 3rd edition. CRC Press, Boca Raton, Florida.
64. Hobbie JE, Daley RJ, Jasper S. 1977. Use of nuclepore filters for counting bacteria by fluorescence microscopy. Appl Environ Microbiol 33:1225–1228. https://doi.org/10.1128/aem.33.5.1225-1228.1977.
65. Miller LG, Baesman SM, Oremland RS. 2015. Stable carbon isotope fractionation during bacterial acetylene fermentation: potential for life detection in hydrocarbon-rich volatiles of icy planet(oid)s. Astrobiology 15:977–986. https://doi.org/10.1089/ast.2015.1355.
66. Sambrook J, Russell DW. 2001. Molecular cloning–a laboratory manual. 3rd ed. Cold Spring Harbor Laboratory, New York, NY.
67. Zimin AV, Marçais G, Puiu D, Roberts M, Salzberg SL, Yorke JA. 2013. The MaSuRCA genome assembler. Bioinformatics 29:2669–2677. https://doi.org/10.1093/bioinformatics/btt476.
68. Walker BJ, Abeel T, Shea T, Priest M, Abouelliel A, Sakthikumar S, Cuomo CA, Zeng Q, Wortman J, Young SK, Earl AM. 2014. Pilon: an integrated tool for comprehensive microbial variant detection and genome assembly improvement. PLoS One 9:e112963. https://doi.org/10.1371/journal.pone.0112963.
69. Tatusova T, DiCuccio M, Badretdin A, Chetvernin V, Nawrocki EP, Zaslavsky L, Lomsadze A, Pruitt KD, Borodovsky M, Ostell J. 2016. NCBI prokaryotic genome annotation pipeline. Nucleic Acids Res 44:6614–6624. https://doi.org/10.1093/nar/gkw569.
70. Cantalapiedra CP, Hernandez-Plaza A, Letunic I, Bork P, Huerta-Cepas J. 2021. eggNOG-mapper v2: functional annotation, orthology assignments, and domain prediction at the metagenomic scale. Mol Biol Evol 38:5825–5829. https://doi.org/10.1093/molbev/msab293.
71. Huerta-Cepas J, Szklarczyk D, Heller D, Hernandez-Plaza A, Forslund SK, Cook H, Mende DR, Letunic I, Rattei T, Jensen LJ, von Mering C, Bork P. 2019. eggNOG 5.0: a hierarchical, functionally and phylogenetically annotated orthology resource based on 5090 organisms and 2502 viruses. Nucleic Acids Res 47:D309–D314. https://doi.org/10.1093/nar/gky1085.
72. Kanehisa M, Furumichi M, Sato Y, Ishiguro-Watanabe M, Tanabe M. 2021. KEGG: integrating viruses and cellular organisms. Nucleic Acids Res 49:D545–D551. https://doi.org/10.1093/nar/gkaa970.
73. Kanehisa M, Sato Y, Morishima K. 2016. BlastKOALA and GhostKOALA: KEGG Tools for Functional Characterization of Genome and Metagenome Sequences. J Mol Biol 428:726–731. https://doi.org/10.1016/j.jmb.2015.11.006.
74. Goris J, Konstantinidis KT, Klappenbach JA, Coenye T, Vandamme P, Tiedje JM. 2007. DNA–DNA hybridization values and their relationship to whole-genome sequence similarities. Int J Syst Evol Microbiol 57:81–91. https://doi.org/10.1099/ijs.0.64483-0.
75. Na S-I, Kim YO, Yoon S-H, Ha S-m, Baek I, Chun J. 2018. UBCG: up-to-date bacterial core gene set and pipeline for phylogenomic tree reconstruction. J Microbiol 56:280–285. https://doi.org/10.1007/s12275-018-8014-6.
76. Drummond A, Ashton B, Buxton S, Cheung M, Cooper A, Duran C, Field M, Heled J, Kearse M, Markowitz S, Moir R, Stones-Havas S, Sturrock S, Thierer T, Wilson A. 2009. Geneious v. 2022.1. Available from http://www.geneious.com/.
77. Nguyen L-T, Schmidt HA, von Haeseler A, Minh BQ. 2015. IQ-TREE: a fast and effective stochastic algorithm for estimating maximum-likelihood phylogenies. Mol Biol Evol 32:268–274. https://doi.org/10.1093/molbev/msu300.
78. Minh BQ, Schmidt HA, Chernomor O, Schrempf D, Woodhams MD, von Haeseler A, Lanfear R. 2020. IQ-TREE 2: new models and efficient methods for phylogenetic inference in the genomic era. Mol Biol Evol 37:1530–1534. https://doi.org/10.1093/molbev/msaa015.
79. Hoang DT, Chernomor O, Haeseler A, Minh BQ, Vinh LS. 2018. UFBoot2: improving the ultrafast bootstrap approximation. Mol Biol Evol 35:518–522. https://doi.org/10.1093/molbev/msx281.
80. NCBI Resource Coordinators. 2016. Database resources of the National Center for Biotechnology Information. Nucleic Acids Res 44:D7–D19. https://doi.org/10.1093/nar/gkv1290.
81. Nordberg H, Cantor M, Dusheyko S, Hua S, Poliakov A, Shabalov I, Smirnova T, Grigoriev IV, Dubchak I. 2014. The genome portal of the Department of Energy Joint Genome Institute: 2014 updates. Nucleic Acids Res 42:D26–D31. https://doi.org/10.1093/nar/gkt1069.
82. Eren AM, Esen ÖC, Quince C, Vineis JH, Morrison HG, Sogin ML, Delmont TO. 2015. Anvi'o: an advanced analysis and visualization platform for 'omics data. PeerJ 3:e1319. https://doi.org/10.7717/peerj.1319.
83. Delmont TO, Eren AM. 2018. Linking pangenomes and metagenomes: the *Prochlorococcus* metapangenome. PeerJ 6:e4320. https://doi.org/10.7717/peerj.4320.
84. Lee I, Ouk Kim Y, Park S-C, Chun J. 2016. OrthoANI: an improved algorithm and software for calculating average nucleotide identity. Int J Syst Evol Microbiol 66:1100–1103. https://doi.org/10.1099/ijsem.0.000760.
85. Roy A, Kucukural A, Zhang Y. 2010. I-TASSER: a unified platform for automated protein structure and function prediction. Nat Protoc 5:725–738. https://doi.org/10.1038/nprot.2010.5.
86. Sutton JM, Baesman SM, Fierst JL, Poret-Peterson AT, Oremland RS, Dunlap DS, Akob DM. 2017. Complete genome sequences of two acetylene fermenting *Pelobacter acetylenicus* strains. Genome Announc 5:e01572-16. https://doi.org/10.1128/genomeA.01572-16.
87. Sutton JM, Baesman SM, Fierst JL, Poret-Peterson AT, Oremland RS, Dunlap DS, Akob DM. 2017. Complete genome sequence of the acetylene fermenting *Pelobacter* strain SFB93. Genome Announc 5:e01573-16. https://doi.org/10.1128/genomeA.01573-16.
88. Lu S, Wang J, Chitsaz F, Derbyshire MK, Geer RC, Gonzales NR, Gwadz M, Hurwitz DI, Marchler GH, Song JS, Thanki N, Yamashita RA, Yang M, Zhang D, Zheng C, Lanczycki CJ, Marchler-Bauer A. 2020. CDD/SPARCLE: the conserved domain database in 2020. Nucleic Acids Res 48:D265–D268. https://doi.org/10.1093/nar/gkz991.
89. Edgar RC. 2004. MUSCLE: multiple sequence alignment with high accuracy and high throughput. Nucleic Acids Res 32:1792–1797. https://doi.org/10.1093/nar/gkh340.
90. Price MN, Dehal PS, Arkin AP. 2009. FastTree: computing large minimum evolution trees with profiles instead of a distance matrix. Mol Biol Evol 26:1641–1650. https://doi.org/10.1093/molbev/msp077.